PAPER

Check for updates

New diterpenoids and sesquiterpenoids from *Siegesbeckia pubescens* Makino and their anti-inflammatory activity

Lingxia Qu, Yuejian Guan, Xinyu Li, Xinning Li, Haixue Kuang, Liu Yang [ID] *
and Hai Jiang [ID] *

Six undescribed terpenoids were isolated from the aboveground parts of *Siegesbeckia pubescens* Makino. These compounds include four diterpenoids (**1–4**) and two sesquiterpenoids (**5–6**), as well as thirteen known compounds (**7–19**). The structures of new compounds were determined through spectroscopic analysis, DP4+ Analysis and ECD calculation. The protective effect of all compounds against lipopolysaccharide (LPS)-induced inflammation in RAW 264.7 cells was tested. The result showed that compounds **2–9**, **12–15** and **17–19** significantly inhibited the production of nitric oxide (NO) in LPS-induced RAW 264.7 cells, among which compound **18** demonstrated the best inhibitory activity against NO release. The potential anti-inflammatory mechanism was investigated through molecular docking. The molecular docking results showed that the active compounds had a strong binding affinity with the key targets. In conclusion, *Siegesbeckia pubescens* Makino has demonstrated multi-component, multi-target and multi-pathway therapeutic characteristics in the treatment of inflammation. These findings provide a valuable theoretical basis for the clinical application of this plant.

1 Introduction

Siegesbeckia herb, derived from the dried aerial parts of *Siegesbeckia orientalis* L., *Siegesbeckia pubescens* Makino or *Siegesbeckia glabrescens* Makino, is a traditional Chinese medicinal plant with documented therapeutic applications.[1] Modern pharmacological studies have identified multiple bioactive compounds in *Siegesbeckia* herb, including sesquiterpenes, diterpenes and flavonoids, which demonstrated promising anti-inflammatory, immune-modulatory and antitumor properties.[2–5]

The medicinal value of this plant prompted us to conduct further phytochemical research on *Siegesbeckia pubescens* Makino, with the aim of discovering new active components. We isolated and identified four undescribed diterpenoids and two undescribed sesquiterpenoids from the plant (Fig. 1), along with 13 known compounds. The chemical structures of these compounds were determined through comprehensive spectroscopic methods such as HR-ESI-MS and 1D/2D NMR, and their absolute configurations were determined by ECD calculation. At the same time, *in vitro* evaluation was conducted to assess the protective effects of these compounds on the inflammatory response of RAW 264.7 cells induced by LPS. The interaction between active small molecules and key targets was studied by molecular docking technology, thereby revealing the potential

Key Laboratory of Basic and Application Research of Beiyao, Heilongjiang University of Chinese Medicine, Ministry of Education, No. 24 Heping Road, Xiangfang, Harbin 150040, China. E-mail: hxk_yl@163.com; jianghai_777@126.com
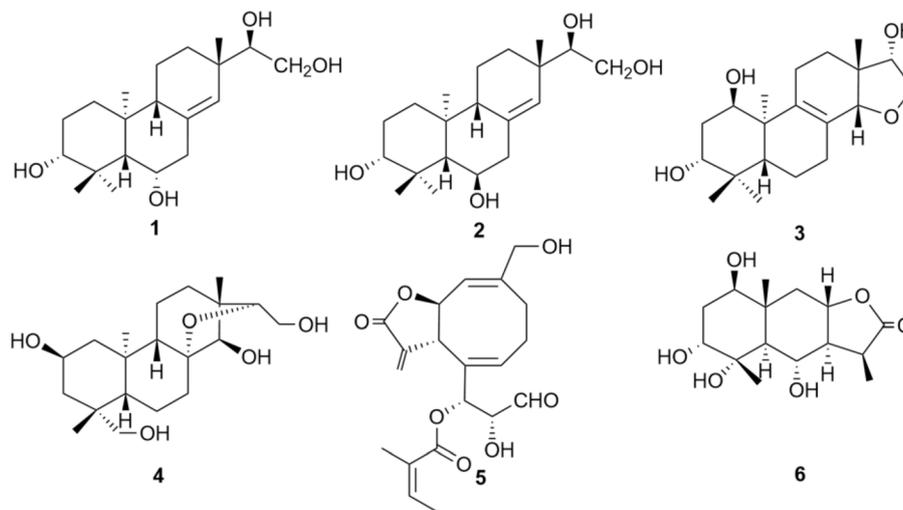
application value of *Siegesbeckia pubescens* Makino in the treatment of inflammation.

2 Results

2.1 Structure elucidation of compounds

Compound **1** was obtained as a white amorphous powder. HR-ESI-MS analysis showed a $[M + NH_4]^+$ ion at m/z 356.2793 (calculated for $C_{20}H_{38}O_4N$, 356.2795) (Fig. S8). The molecular formula was established as $C_{20}H_{34}O_4$ (four degrees of unsaturation) based on combined ^1H-NMR and ^{13}C-NMR data (Table 1). The ^1H-NMR spectrum revealed four singlet methyl groups δ_H 1.24 (3H, s), 1.41 (3H, s), 1.44 (3H, s), 1.76 (3H, s); one olefinic proton δ_H 5.61 (1H, s); three oxygenated methine protons δ_H 3.51 (dt, $J = 11.4$, 4.3 Hz), 4.24 (1H, m), 4.71 (1H, d, $J = 4.1$ Hz) and two oxygenated methylene protons δ_H 4.25 (1H, m), 4.06 (1H, m). The ^{13}C-NMR spectrum displayed twenty carbon signals, including two olefinic carbons at δ_C 131.6 (C-8), 136.6 (C-14); four methyl carbons δ_C 23.7 (C-17), 29.3 (C-18), 18.3 (C-19), 18.6 (C-20), five methines, including three oxygenated carbons at δ_C 79.0 (C-3), 67.8 (C-6), 77.2 (C-15); six methylenes, including one oxygenated methylene at δ_C 64.3 (C-16); and three quaternary carbons as confirmed by HSQC and DEPT experiments. The NMR data of compound **1** resembled those of darutigenol,[4] with the key difference being the presence of a hydroxyl group at C-6 in compound **1** instead of a methylene group, supported by ^1H–^1H COSY correlations between H-6 (δ_H 4.71)/H-5 (δ_H 1.18) and H-7 (δ_H 2.48, 2.63), as well as HMBC

Fig. 1 Chemical structures of compounds **1–6**.

correlations from H$_3$-18 (δ_H 1.44), H$_3$-19 (δ_H 1.76), and H$_3$-20 (δ_H 1.41) to C-6 (δ_C 67.8). The planar structure of compound **1** was established through analysis of HMBC and ^{1}H–^{1}H COSY correlations (Fig. 2).

Furthermore, NOESY correlations between H-5/H-6, H-9 and H$_3$-17, as well as between H$_3$-18/H-3 and H-6, established that H-3, H-5, H-6, H-9, H$_3$-17, and H$_3$-18 were in the β-orientation. The

observed NOESY cross-peaks of H$_3$-20/H-15 and H$_3$-19 indicated the α-orientation of H-15, H$_3$-19, and H$_3$-20 (Fig. 3). The chemical shift value of C-15 is 77.2 ppm, thus the configuration of C-15 is *R* configuration.[3] Quantum chemical computational methods were employed to calculate the ^{13}C NMR chemical shifts of four possible epimers of compound **1**, namely (3*R**,6*S**,15*R*)-**1**, (3*R**,6*R**,15*R*)-**1**, (3*S**,6*S**,15*R*)-**1**, and

Table 1 ^{1}H-NMR (600 MHz) and ^{13}C-NMR (150 MHz) data of compounds **1–3**

No.	**1** (C$_5$D$_5$N) δ_C	δ_H	**2** (C$_5$D$_5$N) δ_C	δ_H	**3** (CD$_3$OD) δ_C	δ_H
1	39.6	1.66 (m)	38.2	1.59 (m)	72.6	3.93 (t, 2.9)
	—	1.23 (m)	—	1.22 (m)	—	—
2	29.0	1.98 (m)	28.6	1.85 (m)	35.6	1.90 (m)
	—	1.92 (m)	—	1.85 (m)	—	1.78 (m)
3	79.0	3.51 (dt,11.4, 4.3)	79.1	3.59 (dd, 11.9, 4.2)	74.2	3.70 (dd, 12.2,4.6)
	—	—	—	—	—	—
4	40.3	—	40.6	—	40.0	—
5	56.9	1.18 (d, 2.0)	60.6	1.45 (dd, 10.5, 3.1)	44.8	1.62 (t, 12.6)
6	67.8	4.71 (d, 4.1)	69.6	4.19 (m)	19.5	1.77 (m)
	—	—	—	—	—	1.56 (m)
7	47.3	2.63 (dt, 14.4, 2.5)	48.4	2.93 (dt, 13.7, 4.1)	31.8	2.36 (m)
	—	2.48 (m)	—	2.57 (t, 12.2)	—	1.93 (m)
8	136.6	—	138.3	—	127.1	—
9	51.8	1.83 (m)	50.8	1.83 (m)	141.6	—
10	38.7	—	39.4	—	43.5	—
11	18.9	1.87 (m)	19.3	1.61 (m)	21.5	2.32 (m)
	—	1.63 (m)	—	1.55 (m)	—	2.08 (dd, 17.3, 2.8)
12	33.2	2.50 (m)	33.4	2.51 (dd, 12.7, 3.6)	30.6	1.34 (m)
	—	1.21 (m)	—	1.15 (m)	—	1.28 (dd, 12.3, 4.3)
13	40.9	—	38.5	—	44.3	—
14	131.6	5.61 (s)	130.2	5.53 (s)	84.3	3.56 (m)
15	77.2	4.24 (m)	76.8	4.11 (d, 9.1)	80.7	3.79 (dd, 2.4, 5.2)
16	64.3	4.25 (m)	64.4	4.21 (m)	74.7	4.20 (dd, 9.8, 5.2)
	—	4.06 (m)	—	4.05 (m)	—	3.57 (m)
17	23.7	1.24 (s)	23.6	1.20 (s)	14.9	0.96 (s)
18	29.3	1.44 (s)	32.7	1.98 (s)	28.7	1.04 (s)
19	18.3	1.76 (s)	17.1	1.49 (s)	16.3	0.82 (s)
20	18.6	1.41 (s)	16.6	0.82 (s)	20.8	1.01 (s)
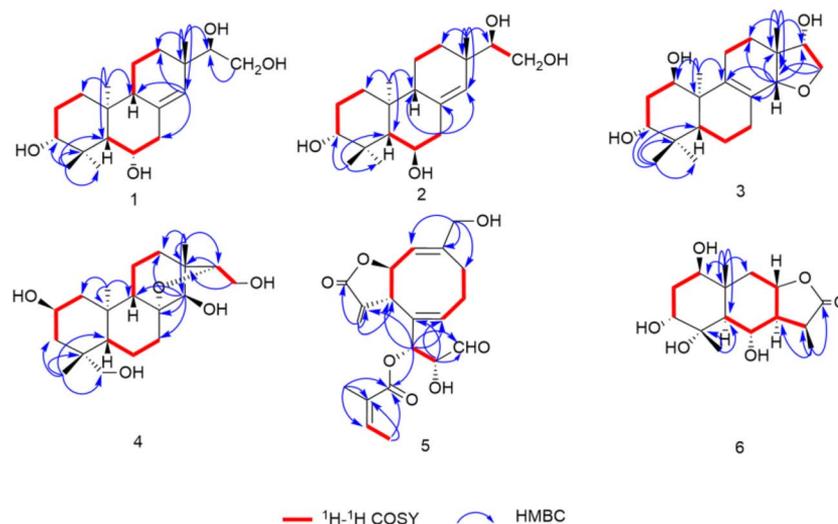
Fig. 2 Key HMBC and ^{1}H–^{1}H COSY of compounds **1–6**.

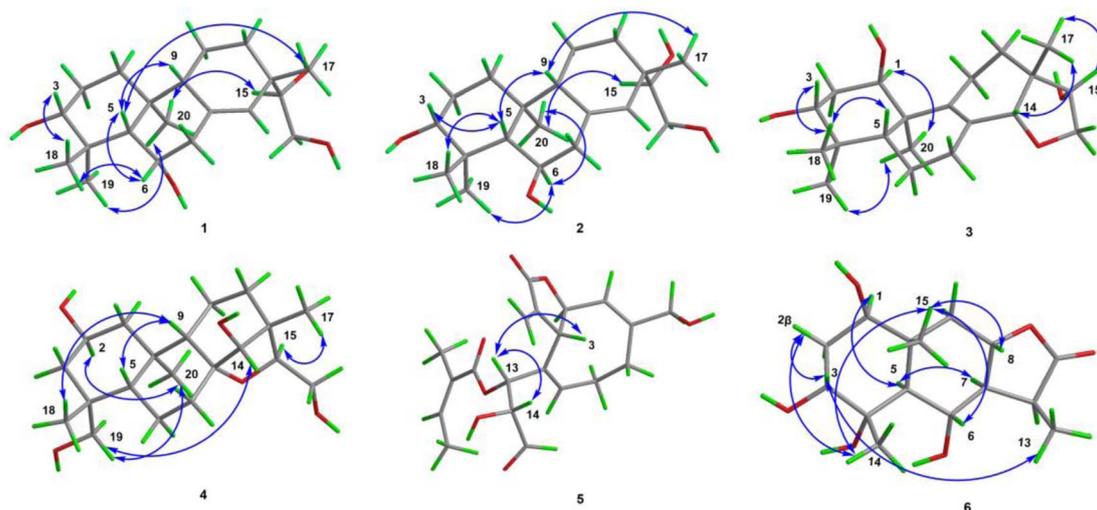**Fig. 3** NOESY correlations of compounds **1–6**.

(3S*,6R*,15R)-**1**. As shown in Fig. S48, the calculated ^{13}C NMR chemical shifts of the (3R*,6S*,15R)-**1** exhibited excellent agreement with the experimental data, with a correlation coefficient (R^2) of 0.9946. Meanwhile, the mean absolute error (MAE) and corrected mean absolute error (CMAE) were 1.7 and 2.5, Furthermore, DP4+ probability analysis strongly confirmed this epimer as the true relative configuration, with a DP4+ probability of 100% (Fig. S49). Based on the comprehensive analysis, the relative configuration of compound **1** was determined. Through comparative analysis of experimental and calculated ECD spectra (Fig. 4), the absolute configuration of compound **1** was established as 3R,6S,15R. Finally, compound **1** was identified and named as *ent*-3α,6α,15,16-tetrahydroxypimar-8(14)-ene.

Compound **2** was obtained as a white amorphous powder. HR-ESI-MS analysis showed a [M + NH$_4$]$^+$ ion at *m/z* 356.2794 (calculated for $C_{20}H_{38}O_4N$, 356.2795), establishing the same molecular formula ($C_{20}H_{34}O_4$) as compound **1** (Fig. S16). Comparative analysis of 1D and 2D NMR data revealed that compound **1** and **2** share the same planar structure but differ in their C-6 configurations. NOESY correlations between H-6/H$_3$-19 and H$_3$-20 confirmed the β-orientation of H-6 (Fig. 3). By comparing the specific optical rotation of compound **2** and compound **1**, it was found that the magnitudes of their specific optical rotations were equal while the signs were opposite.

Further support for the authentic configuration of this compound as 3R,6R,15R was provided by quantum chemical calculations and DP4+ probability analysis, with the DP4+ probability reaching 97.53% (Fig. S50 and S51). Finally, compound **2** was identified and named as *ent*-3α,6β,15,16-tetrahydroxypimar-8(14)-ene.

Compound **3** was obtained as a white amorphous powder. HR-ESI-MS analysis showed a [M + H]$^+$ ion at *m/z* 337.2376 (calculated for $C_{20}H_{33}O_4$, 337.2373) (Fig. S24). Combined ^{1}H-
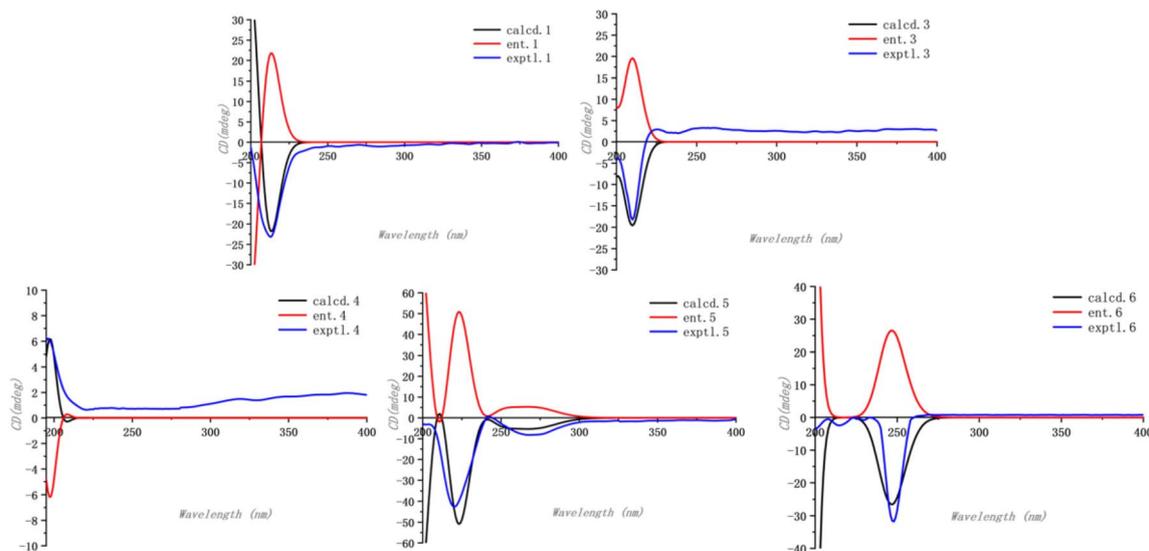
Fig. 4 Experimental and calculated ECD spectra of compounds **1** and **3–6**.

NMR and ^{13}C-NMR data established the molecular formula as $C_{20}H_{32}O_4$ with five degrees of unsaturation (Table 1). The ^{1}H-NMR spectrum exhibited four singlet methyl groups δ_H 0.82 (3H, s), 0.96 (3H, s), 1.01 (3H, s), 1.04 (3H, s), four oxygenated methine protons δ_H 3.56 (1H, m), 3.70 (1H, dd, J = 12.2, 4.6 Hz), 3.79 (1H, dd, J = 2.4, 5.2 Hz), 3.93 (1H, t, J = 2.9 Hz), and two oxygenated methylene protons δ_H 3.57 (1H, m), 4.20 (1H, dd, J = 9.8, 5.2 Hz). The HSQC and DEPT spectrum confirmed the existence of five quaternary carbons, including two alkenyl carbon signals at δ_C 127.1 (C-8) and 141.6 (C-9); four methyls at δ_C 14.9 (C-17), 28.7 (C-18), 16.3 (C-19), 20.8 (C-20); five methines, including four oxygenated carbons at δ_C 72.6 (C-1), 74.2 (C-3), 84.3 (C-14), 80.7 (C-15), and six methylenes, including one oxygenated methylene δ_C 74.7 (C-16). The spectroscopic data resembled those of ent-14β,16-epoxy-8-pimarene-3β,15α-diol,[6] with the key difference being a hydroxyl group at C-1 in compound **3** instead of a methylene group supported by ^{1}H–^{1}H COSY correlations of H-1 (δ_H 3.93), H-3 (δ_H 3.70)/H-2 (δ_H 1.78, 1.90) and HMBC correlations from H$_3$-20 (δ_H 1.01) to C-1 (δ_C 72.6). The planar structure of compound **3** was established through HMBC and ^{1}H–^{1}H COSY correlations (Fig. 2).

NOESY correlations between H$_3$-18/H-3, H-5; H$_3$-17/H-14, H-15 confirmed the β-orientation of H-3, H-5, H-14, H-15, H$_3$-17 and H$_3$-18, while correlations H$_3$-20/H-1, H$_3$-19 established the α-orientation of H-1, H$_3$-19 and H$_3$-20 (Fig. 3). The chemical shift value of C-15 is 80.7 ppm, thus the configuration of C-15 is S configuration.[3] Quantum chemical calculations predicted the ^{13}C NMR chemical shifts of four stereoisomers of compound **3**: (1R*,3R*,15S)-**3**, (1R*,3S*,15S)-**3**, (1S*,3S*,15S)-**3**, and (1S*, 3R*,15S)-**3**. As shown in Fig. S52, (1R*,3R*,15S)-**3** exhibited excellent agreement between calculated and experimental ^{13}C NMR data (R^2 = 0.9921, MAE = 2.1, CMAE = 0.7). DP4+ analysis further confirmed this as the authentic configuration (99.99% probability, Fig. S53), establishing the relative configuration. Comparative analysis of experimental and computed ECD spectra (Fig. 4) assigned the absolute configuration of compound **3** as 1R,3R,15S. Consequently, compound **3** was identified and designated as 14α,16-epoxy-ent-1β,3α,15,16-trihydroxypimar-8-ene.

Compound **4** was obtained as a white amorphous powder. HR-ESI-MS analysis exhibited a peak at m/z 399.2393 [M + HCOO]$^-$ (calcd for $C_{21}H_{35}O_7$, 399.2388) (Fig. S32). Combined with ^{1}H-NMR and ^{13}C-NMR data, the molecular formula was determined to be $C_{20}H_{34}O_5$, with four degrees of unsaturation (Table 2). The ^{1}H-NMR spectrum revealed three singlet methyl signals at δ_H 1.19 (3H, s), 1.29 (3H, s), and 1.29 (3H, s); three oxygenated methine proton signals at δ_H 4.31 (1H, m), 4.18 (1H, m), and 3.60 (1H, d, J = 4.4 Hz); and four oxygenated methylene proton signals at δ_H 4.30 (1H, m), 4.14 (1H, d, J = 10.2 Hz), 4.19 (1H, m), and 3.76 (1H, d, J = 11.5 Hz). The ^{13}C-NMR spectrum displayed twenty carbon signals, and HSQC and DEPT experiments confirmed the presence of three methyl carbons at δ_C 21.8 (C-17), 28.7 (C-18), and 18.1 (C-20); five methine carbons, including three oxygenated methines at δ_C 63.9 (C-2), 82.3 (C-14), and 86.3 (C-15); eight methylene carbons, including two oxygenated methylenes at δ_C 62.3 (C-16) and 65.4 (C-14); and four quaternary carbons. The NMR data of compound **4** is similar to that of ent-8,15-epoxy-2α,16,19-trihydroxy-pimarane[7] isolated in this study. The difference lies in that compound **4** has a hydroxyl group attached at the C-14 position, replacing the previous methylene signal. This is supported by the correlation in the HMBC spectrum from H-14 (δ_H 3.60) to C-7 (δ_C 37.7), C-8 (δ_C 82.0), C-9 (δ_C 47.7), C-12 (δ_C 26.7), C-17 (δ_C 21.8). The correlations of HMBC and ^{1}H–^{1}H COSY spectrum revealed the planar structure of compound **4** (Fig. 2).

Furthermore, the correlations of H-5/H-9, H$_3$-18; H-15/H$_3$-17 in the NOESY spectrum indicated that H-5, H-9, H-15, H$_3$-17 and H$_3$-18 were located on the same side of the ring and were in the β orientation. The correlations of H$_2$-19/H-14, H$_3$-20; H-2/H$_3$-20 suggested that H-2, H-14, H$_2$-19 and H$_3$-20 were in the

Table 2 ^{1}H-NMR (600 MHz) and ^{13}C-NMR (150 MHz) data of compounds **4–6**

No.	4 (C$_5$D$_5$N) δ_C	4 δ_H	5 (CD$_3$OD) δ_C	5 δ_H	6 (CD$_3$OD) δ_C	6 δ_H
1	51.0	2.37 (d, 11.4)	171.5	—	73.7	3.82 (dd, 11.5, 4.7)
	—	1.31 (m)	—	—	—	—
2	63.9	4.31 (m)	137.2	—	34.3	1.87 (m)
	—	—	—	—	—	1.87 (m)
3	46.2	2.92 (dd, 12.5, 3.6)	52.4	2.85 (m)	75.7	3.54 (t, 2.8)
	—	1.32 (m)	—	—	—	—
4	41.5	—	75.9	5.27 (t, 10.2)	75.4	—
5	56.1	1.26 (t, 7.3)	129.5	5.11 (d, 10.2)	51.7	1.88 (m)
6	20.1	1.82 (m)	142.6	—	71.8	4.20 (t, 10.1)
	—	1.82 (m)	—	—	—	—
7	37.7	2.12 (m)	33.1	2.83 (m)	61.1	1.74 (m)
	—	1.96 (dd, 13.8, 2.7)	—	2.01 (td, 12.8, 1.6)	—	—
8	82.0	—	27.9	2.66 (m)	78.0	4.05 (m)
	—	—	—	2.52 (m)	—	—
9	47.7	2.05 (m)	157.6	6.76 (dd, 10.2, 7.4)	44.6	2.32 (dd, 11.3, 3.8)
	—	—	—	—	—	1.35 (d, 11.8)
10	39.1	—	146.1	—	42.1	—
11	19.7	1.78 (m)	121.6	6.16 (d, 3.4)	42.6	2.66 (d, 12.0, 6.9)
	—	1.64 (m)	—	5.75 (d, 3.4)	—	—
12	26.7	2.09 (m)	60.5	4.45 (brd, 13.0)	182.0	—
	—	1.52 (m)	—	4.19 (brd, 13.0)	—	—
13	42.7	—	72.0	6.62 (dd, 8.6, 1.5)	14.9	1.30 (d, 6.9)
14	82.3	3.60 (d, 4.4)	70.0	4.13 (dd, 8.6, 1.9)	16.6	0.97 (s)
15	86.3	4.18 (m)	197.3	9.45 (d, 2.0)	23.3	1.32 (s)
16(1′)	62.3	4.30 (m)	168.6	—	—	—
	—	4.14 (d, 10.2)	—	—	—	—
17(2′)	21.8	1.19 (s)	129.1	—	—	—
18(3′)	28.7	1.29 (s)	139.5	6.13 (m)	—	—
19(4′)	65.4	4.19 (m)	21.0	1.91 (p, 1.5)	—	—
	—	3.76 (d, 11.5)	—	—	—	—
20(5′)	18.1	1.29 (s)	16.2	1.98 (dq, 1.5, 7.2)	—	—

α orientation (Fig. 3). The chemical shift value of C-15 is 86.3 ppm, thus the configuration of C-15 is *S* configuration.[3] Quantum chemical calculations predicted the ^{13}C NMR chemical shifts of four stereoisomers of compound **4**: (2*S**,14*R**,15*S*)-**4**, (2*R**,14*R**,15*S*)-**4**, (2*R**,14*S**,15*S*)-**4** and (2*S**,14*S**,15*S*)-**4**. As shown in Fig. S54, the calculated ^{13}C NMR chemical shifts of (2*S**,14*R**,15*S*)-**4** were in good agreement with experimental data, with R^2 = 0.9867, MAE = 1.9 and CMAE = 2.5. Further DP4+ probability analysis confirmed this as the authentic configuration (100.00% probability, Fig. S55), establishing the relative configuration of compound **4**. Finally, comparative analysis of experimental and calculated ECD spectra (Fig. 4) determined the absolute configuration of compound **4** as 2*S*,14*R*,15*S*. Finally, compound **4** was identified and named as 8,15-epoxy-*ent*-2β,14β,16,19-tetrahydroxy-pimarane.

Compound **5** was isolated as a white amorphous powder. HR-ESI-MS analysis showed a peak at *m/z* 377.1591 [M + H]$^+$ (calculated for C$_{20}$H$_{25}$O$_7$, 377.1595) (Fig. S40). The molecular formula was determined to be C$_{20}$H$_{24}$O$_7$ with seven degrees of unsaturation, based on combined ^{1}H-NMR and ^{13}C-NMR data (Table 2). The ^{1}H-NMR spectrum exhibited characteristic signals including one aldehyde proton at δ_H 9.45 (1H, d, *J* = 2.0 Hz); two methyl groups at δ_H 1.91 (3H, p, *J* = 1.5 Hz) and 1.98 (3H, dq, *J* = 1.5, 7.2 Hz); five olefinic protons at δ_H 6.76 (1H, dd, *J* = 10.2, 7.4 Hz), 6.13 (1H, m), 6.16 (1H, d, *J* = 3.4 Hz), 5.75 (1H, d, *J* = 3.4 Hz), 5.11 (1H, d, *J* = 10.2 Hz); two oxygenated methine protons at δ_H 4.13 (1H, dd, *J* = 8.6, 1.9 Hz) and 6.62 (1H, dd, *J* = 8.6, 1.5 Hz); and two oxygenated methylene protons at δ_H 4.45 (1H, brd, *J* = 13.0 Hz) and 4.19 (1H, brd, *J* = 13.0 Hz). The ^{13}C-NMR spectrum and DEPT spectrum revealed twenty carbon signals, including two methyl carbons at δ_C 21.0 (C-4′), 16.2 (C-5′); three carbonyl carbons at δ_C 171.5 (C-1), 197.3 (C-15), 168.6 (C-1′); eight olefinic carbons at δ_C 137.2 (C-2), 129.5 (C-5), 142.6 (C-6), 157.6 (C-9), 146.1 (C-10), 121.6 (C-11), 129.1 (C-2′), 139.5 (C-3′), three methylene carbons including one oxygenated methylene at δ_C 60.5 (C-12); and four methine carbons, including three oxygen-containing methylene signals δ_C 75.9 (C-4), 72.0 (C-13), 70.0 (C-14). The spectral data of compound **5** is similar to siegenolide A8 except for the replacement of a methoxy group with a hydroxyl group at C-14. This was supported by correlation of H-13 (δ_H 6.62)/H-14 (δ_H 4.13) in the ^{1}H–^{1}H COSY spectrum and the absence of the methoxy signal in the ^{1}H-NMR. The planar structure of compound **5** was established through HMBC and ^{1}H–^{1}H COSY correlations (Fig. 2).

Furthermore, NOESY correlations between H-13/H-3 and H-14 indicated that these protons are cofacial, adopting a β-orientation. Quantum chemical calculations were employed to

predict the ^{13}C NMR chemical shifts of two candidate isomers, (3R^*,4S^*,13R^*,14R^*)-**5** and (3S^*,4R^*,13R^*,14R^*)-**5**. As shown in Fig. S56, the calculated ^{13}C NMR data of (3R^*,4S^*, 13R^*,14R^*)-**5** were in good agreement with the experimental results, with an R^2 value of 0.9776, a MAE of 4.4 and a CMAE of 2.3. Further DP4+ probability analysis corroborated this structure as the correct relative configuration, yielding a DP4+ probability of 99.53% (Fig. S57). Combined with the experimental and calculated ECD spectra comparison (Fig. 4), the absolute configuration of compound **5** was ultimately assigned as 3R,4S,13R,14R. Finally, compound **5** was identified and named siegenolide C.

Compound **6** was obtained as a white amorphous powder. HR-ESI-MS analysis showed a [M + H]$^+$ ion at m/z 301.1647 (calcd for $C_{15}H_{25}O_6$, 301.1646) (Fig. S47). The molecular formula was established as $C_{15}H_{24}O_6$ (four degrees of unsaturation) based on ^{1}H and ^{13}C NMR data (Table 2). The ^{1}H-NMR spectrum revealed three methyl signals at 0.97 (3H, s), 1.30 (3H, d, J = 6.9 Hz), 1.32 (3H, s), along with four oxygenated methine protons at δ_H 3.54 (t, J = 2.8 Hz), 3.82 (dd, J = 11.5, 4.7 Hz), 4.05 (m), and 4.20 (t, J = 10.1 Hz). The ^{13}C NMR spectrum displayed fifteen carbon signals, including three methyls at δ_C 14.9 (C-13), 23.3 (C-14), 16.6 (C-15), seven methines included four oxygenated at δ_C 73.7(C-1), 75.7 (C-3), 71.8 (C-6), 78.0 (C-8), two methylene, and three quaternary carbons (one carbonyl at δ_C 182.0), as confirmed by HSQC experiments. The spectral data of compound **6** were similar to those of Inujaponin E,[9] indicating that this compound is an eudesmane-type sesquiterpene lactone derivative. The key difference was the presence of hydroxyl groups at C-3 and C-6, replacing the original methylene groups. ^{1}H–^{1}H COSY correlations between H-2 (δ_H 1.87)/H-1 (δ_H 3.82), H-3 (δ_H 3.54); H-6 (δ_H 4.20)/H-5 (δ_H 1.88), H-7 (δ_H 1.74) confirmed the hydroxyl at C-3 and C-6. The planar structure of compound **6** was established through HMBC and ^{1}H–^{1}H COSY correlations (Fig. 2).

Furthermore, the correlations in the NOESY spectrum of H$_3$-14/H-6, H-8, H$_3$-15; H-2β/H-3, H$_3$-13, H$_3$-15 indicated that H-3, H-6, H-8, H$_3$-13, H$_3$-14, and H$_3$-15 were located on the same side of the ring, indicating a β orientation. The correlations of H-5/H-1 and H-7 indicated that H-1, H-5, and H-7 were in an α orientation (Fig. 3). Quantum chemical calculations were employed to predict the ^{13}C NMR chemical shifts of eight candidate isomers: (3R^*,6S^*,8S^*)-**6**, (3S^*,6S^*,8S^*)-**6**, (3R^*,

6R^*,8S^*)-**6**, (3R^*,6S^*,8R^*)-**6**, (3S^*,6S^*,8R^*)-**6**, (3S^*,6R^*,8S^*)-**6**, (3R^*,6R^*,8R^*)-**6**, and (3S^*,6R^*,8R^*)-**6**. As shown in Fig. S58, the calculated ^{13}C NMR chemical shifts of (3R^*,6S^*,8S^*)-**6** were in good agreement with the experimental data, with an R^2 value of 0.9975, a MAE of 1.6 and a CMAE of 0.5. Further DP4+ probability analysis corroborated this structure as the correct relative configuration, with a DP4+ probability of 100.00% (Fig. S59). Combined with the comparison of experimental and calculated ECD spectra (Fig. 4), the absolute configuration of compound **6** was assigned as 3R,6S,8S. Finally, compound **6** was identified and named as 1β,3α,4α,6α-tetrahydroxy-11aH-eudesma-12,8α-olide.

The other compounds were identified as siegeside A (**7**),[10] siegesbeckianal (**8**),[11] ent-2α,15R,16,19-tetrahydroxypimar-8 (14)-ene (**9**),[12] 2-oxo-15,16,19-trihydroxy-ent-pimar-8(14)-ene (**10**),[13] ent-12α,16-epoxy-2β,15α,19-trihydroxypimar-8-ene (**11**),[13] ent-12α,16-epoxy-2β,15α,19-trihydroxypimar-8(14)-ene (**12**),[13] siegesbeckia E (**13**),[3] ent-3α15,16,19-tetrahydroxypimar-8(14)-ene(**14**),[14] 14β,16-epoxy-ent-3β,15α,19-trihydroxypimar -7-ene(**15**),[12] (4R,5S,7S,8R,9S,10S,13R,16R)-7,17-dihydroxy kauran-19-oic acid (**16**),[15] (4S,7R,8R,10S,11S)-11α,13-dihydro-4H-xan-thalongi-4-O-β-D-glucopyranoside (**17**),[16] siegenolide B (**18**),[8] siegesbeckialide J (**19**)[17] from their NMR data comparison with reported in the literature.

2.2 Evaluation of anti-inflammatory activities

The inhibitory effect of compounds **1** to **19** on the production of NO by LPS-activated RAW 264.7 cells was tested. Within the concentration range of 50 μM, no significant cytotoxicity of these compounds was detected by the MTT assay. Subsequently, the evaluation was conducted at the above-mentioned maximum safe concentration. The result showed that compounds **2–9**, **12–15** and **17–19** could significantly inhibit the production of NO at 50 μM, among which compound **18** demonstrated the best inhibitory activity against NO release (Fig. 5).

2.3 Predicted binding modes of compounds and iNOS, COX-2 using molecular docking analysis

iNOS and COX-2 are key enzymes involved in inflammatory processes. iNOS catalyzes the production of nitric oxide from L-arginine and is implicated in the development of various
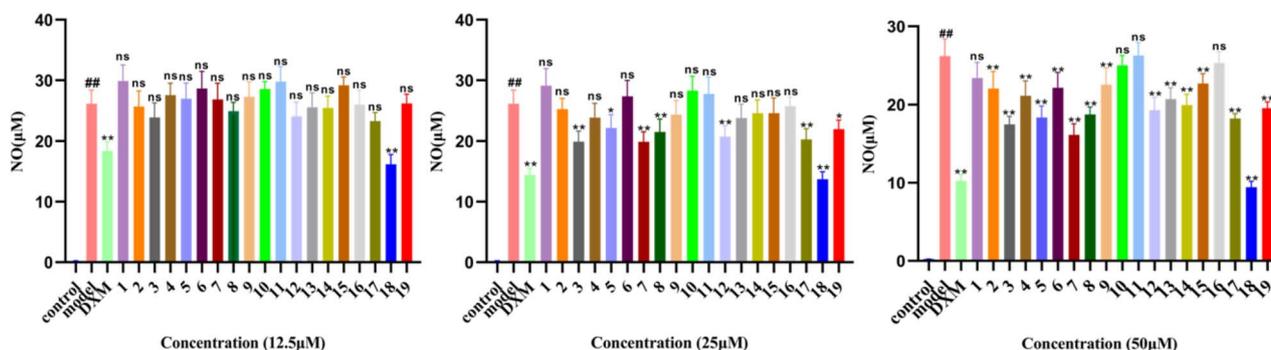

Fig. 5 The NO production induced by LPS in RAW 264.7 cells of **1–19**.

inflammatory diseases. COX-2 plays a significant role in initiating inflammatory responses and contributing to tissue damage. Consequently, inhibiting the activity of iNOS and COX-2 represents a strategic approach for treating inflammatory disorders.[2]

The compounds (**3, 5, 7, 17, 18**) were subjected to molecular docking. The results of the molecular docking study indicated that compounds **3, 5, 17,** and **18** had strong interactions with the iNOS protein, and compounds **3, 5, 7, 17,** and **18** had strong interactions with the COX-2 protein (S82–S90). Detailed information on the specific binding residues and the logarithms of free binding energies was collated in Tables S3 and S4.

3 Materials and methods

3.1 General experimental procedures

Silica gel (200–300 mesh, Qingdao Marine Chemical Factory, Qingdao, China), MCI gel (CHP20P, Mitsubishi Chemical Corporation, Tokyo, Japan) and ODS (50 μm, YMC, Kyoto, Japan) were used for column chromatography. Semi-preparative HPLC was performed on a Shimadzu LC-6AD liquid chromatography with a C18 column (10 mm × 250 mm, 5 μm, YMC). NMR spectra were determined by Bruker Avance III 600 (Germany, Bruke), HR-ESI-MS data were obtained from Agilent 6546 LC-Q-TOF (USA, Agilent); optical rotation was recorded by JASCO P-2000 polarimeter (Japan, JASCO); ECD spectra were determined by Biologic MOS-450 (France, Biologic). RAW 264.7 cells (STCC20020P-1, Wuhan Servicebio Technology Co., Ltd, China).

3.2 Plant material

The dried aerial parts of *Siegesbeckia pubescens* Makino were purchased from Bozhou Medicinal Materials Market in Anhui Province and it was identified by Professor Guo Shenglei of Heilongjiang University of Chinese Medicine. The voucher specimen (no. 2023712-1) is stored in the same institution.

3.3 Separation

Dried *Siegesbeckia pubescens* Makino (5.0 kg) was extracted three times with 75% ethanol for 2 hours each time. The combined filtrate was concentrated under reduced pressure to obtain the ethanol extract. The extract was suspended in water and extracted with petroleum ether, yielding 150.0 g of petroleum ether-soluble fraction and 450.0 g of water-soluble fraction.

The water layer (450.0 g) was fractionated by silica gel column chromatography using a gradient elution of CH_2Cl_2–MeOH (100 : 0 to 100 : 50), yielding nine fractions (Fr. A–Fr. I). Fr. B (20.5 g) was further purified by silica gel column chromatography with a gradient of CH_2Cl_2–MeOH (100 : 10 to 100 : 20), affording four subfractions (Fr. B-1 to Fr. B-4). Fr. B-2 was subjected to ODS reverse-phase column chromatography using a MeOH–water gradient (100 : 20 to 100 : 0), yielding five fractions (Fr. B2-1 to Fr. B2-5). Fr. B2-3 was isolated by semi-preparative HPLC with methanol–water solvent system (70 : 30), yielding compounds **8** (4.9 mg), **10** (6.4 mg), **16** (7.0 mg), and **18** (2.3 mg).

Fraction D (20.5 g) was separated by ODS reverse-phase column chromatography using a MeOH–water gradient (10 : 90 to 100 : 0), yielding five subfractions (Fr. D-1 to Fr. D-5). Fr. D-3 was further purified by semi-preparative HPLC with MeOH–water (32 : 68), affording compounds **13** (7.8 mg), **14** (5.0 mg), and **15** (8.7 mg). Fr. D-4 (3.3 g) was fractionated *via* MCI reverse-phase column chromatography with a MeOH–water gradient (30 : 70 to 100 : 0), resulting in four subfractions (Fr. D4-1 to Fr. D4-4). Fr. D4-3 was isolated by semi-preparative HPLC using MeOH–water system (60 : 40), yielding compounds **3** (4.5 mg), **6** (3.0 mg), and **19** (6.0 mg).

Fraction E (40.0 g) was subjected to ODS reverse-phase column chromatography with a MeOH–water gradient (10 : 90 to 100 : 0), yielding six fractions (Fr. E-1 to Fr. E-6). Fr. E-2 was purified by semi-preparative HPLC eluted with MeOH–water (50 : 50), obtaining compounds **1** (4.5 mg), **2** (4.2 mg), **7** (7.8 mg), **9** (10.4 mg), and **11** (8.7 mg). Further purification of Fr. E-3 by semi-preparative HPLC with MeOH–water (58 : 42) yielded compounds **4** (3.0 mg), **5** (4.0 mg), **12** (5.2 mg), and **17** (5.0 mg).

3.3.1 *ent*-3α,6α,15,16-tetrahydroxypimar-8(14)-ene. White amorphous powder; $[\alpha]_D25 = +20.0$, ($c = 0.1$, MeOH); HR-ESI-MS: m/z 356.2793 $[M + NH_4]^+$ (calcd for 356.2795), ^{1}H-NMR and ^{13}C-NMR (C_5D_5N, 600, 150 MHz) data, see Table 1.

3.3.2 *ent*-3α,6β,15,16-tetrahydroxypimar-8(14)-ene. White amorphous powder; $[\alpha]_D^{25} = -20.0$, ($c = 0.1$, MeOH); HR-ESI-MS: m/z 356.2794 $[M + NH_4]^+$ (calcd for 356.2795), ^{1}H-NMR and ^{13}C-NMR (C_5D_5N, 600, 150 MHz) data, see Table 1.

3.3.3 14α,16-epoxy-*ent*-1β,3α,15,16-trihydroxypimar-8-ene. White amorphous powder; $[\alpha]_D^{25} = -10.0$, ($c = 0.1$, MeOH); HR-ESI-MS: m/z 337.2376 $[M + H]^+$ (calcd for 337.2373), ^{1}H-NMR and ^{13}C-NMR (CD_3OD, 600, 150 MHz) data, see Table 1.

3.3.4 8,15-epoxy-*ent*-2β,14β,16,19-tetrahydroxy-pimarane. White amorphous powder; $[\alpha]_D^{25} = -10.0$, ($c = 0.1$, MeOH); HR-ESI-MS: m/z 399.2393 $[M + HCOO]^-$ (calcd for 399.2388), ^{1}H-NMR and ^{13}C-NMR (C_5D_5N, 600, 150 MHz) data, see Table 2.

3.3.5 Siegenolide C. White amorphous powder; $[\alpha]_D^{25} = -20.0$, ($c = 0.1$, MeOH); HR-ESI-MS: m/z 377.1591 $[M + H]^+$ (calcd for 377.1595), ^{1}H-NMR and ^{13}C-NMR (CD_3OD, 600, 150 MHz) data, see Table 2.

3.3.6 1β,3α,4α,6α-tetrahydroxy-11aH-eudesma-12,8α-olide. White amorphous powder; $[\alpha]_D^{25} = -20.0$, ($c = 0.1$, MeOH); HR-ESI-MS: m/z 301.1647 $[M + H]^+$ (calcd for 301.1646), ^{1}H-NMR and ^{13}C-NMR (CD_3OD, 600, 150 MHz) data, see Table 2.

3.4 NMR chemical shift calculation and DP4+ probability analysis

Initially, conformational space exploration was performed using SPARTAN software, where semi-empirical PM6 methodology was employed to conduct a global conformational search for potential isomers of the target compound. Subsequently, density functional theory (DFT) geometry optimization was executed for all low-energy conformers in Gaussian 09,[18] utilizing the B3LYP functional and 6-31G(d) basis set as the computational benchmark. The reliability of potential energy minima was verified *via* vibrational frequency analysis (absence of imaginary frequencies). To enhance energy evaluation

accuracy, single-point Gibbs free energy calculations were performed for each conformer using the M062X functional combined with the 6-311+G(2d,p) basis set, and dominant conformers (>5% population at 298.15 K) were selected based on Boltzmann distribution.

NMR parameters were computed using the gauge-independent atomic orbital (GIAO) method at the mPW1PW91//6-31+G(d,p) theoretical level. To simulate solvation effects, a self-consistent reaction field (SCRF) implicit solvent model was incorporated, specifically parameterized for the dielectric environment of MeOH. The agreement between calculated and experimental chemical shifts was systematically evaluated through multi-dimensional metrics, including linear correlation coefficient (R^2), mean absolute error (MAE), corrected mean absolute error (CMAE), and DP4+ probability analysis.[19]

3.5 ECD calculation

The theoretical calculations of **1–6** were performed using Gaussian 09. The possible conformations were initially obtained from the program Spartan 14 and then optimized at B3LYP/6-31G(d) level in the gas phase. Room-temperature equilibrium populations were calculated according to the Boltzmann distribution law. The ECD calculations were performed using Time Dependent Density Functional Theory (TDDFT) at wB97xd/6-311G(d,p) level in methanol with PCM model. The calculated ECD spectra were obtained by weighing the Boltzmann distribution rate of each geometric conformation, and the sigma/gamma value for processing the calculated ECD was 0.3 eV. All calculated curves were shifted +25 nm to better simulate experimental spectra.

3.6 Anti-inflammatory activity assay

The anti-inflammatory effects of the compounds were evaluated *in vitro* by measuring nitric oxide (NO) production in LPS-induced RAW 264.7 cells. RAW 264.7 cells in the logarithmic growth phase were seeded into 96-well plates at a density of 2×10^5 cells per well and cultured for 24 h. The experiment included three groups: blank control, LPS group (1 μg mL^{-1}), and LPS (1 μg mL^{-1}) + compound group (12.5, 25, 50 μM). Dexamethasone was as the positive control. After 24 h of incubation, the cell supernatant was collected for further analysis. NO levels in RAW 264.7 cells were measured using the Griess reagent assay. Briefly, 50 μL of supernatant was mixed with 50 μL of Griess Reagent I and II in 96-well plate. Absorbance at 540 nm was measured at room temperature, and NO concentrations were calculated based on a standard curve.[11,20]

3.7 Molecular docking studies

The three-dimensional crystal structures of iNOS (PDB ID: 3EJ8) and COX-2 (PDB ID: 1CX2) were obtained from the RCSB Protein Data Bank. Candidate compounds underwent structural optimization using Chem 3D software and were subsequently exported as PDB files for molecular docking. Molecular docking was performed using AutoDock to identify the most favorable binding conformation for each compound. Three-dimensional visualization of docking results was conducted using PyMOL.

4 Conclusion

In summary, we isolated 19 terpenoids from the aerial parts of *Siegesbeckia pubescens* Makino, including six novel compounds. Notably, compounds **2–9**, **12–15**, and **17–19** exhibited significant anti-inflammatory activity. The results of molecular docking revealed the initial anti-inflammatory mechanism of bioactive terpenoids binding to iNOS/COX-2. Our study expanded the material basis of the terpenoid chemical components of this plant species, revealed the potential application of *Siegesbeckia pubescens* Makino as a therapeutic agent for inflammation.

Author contributions

L. X. Qu: writing–original draft, investigation, formal analysis, Y. J. Guan: investigation, formal analysis, data curation. X. Y. Li: visualization, investigation, data curation. X. N. Li: data curation. H. X. Kuang: project administration. L. Yang: editing, supervision, project administration, funding acquisition. H. Jiang: editing, supervision, project administration, funding acquisition, conceptualization.

Conflicts of interest

There are no conflicts to declare.

Data availability

The raw data supporting the conclusions will be made available by the authors upon request.

Supplementary information (SI): original NMR data of all compounds, DP4+ analysis results, cellular activity data, and molecular docking results. See DOI: https://doi.org/10.1039/d5ra08807k.

Acknowledgements

References

1 The State Commission of Chinese Pharmacopoeia, *Chinese Pharmacopoeia*, China Medical Science Press, 2025.

2 Y. Y. Zheng, Z. F. Guo, H. Chen, T. R. G. Bao, X. X. Gao, A. H. Wang and J. M. Jia, *Phytochemistry*, 2023, **205**, 113503.

3 X. X. Gao, Z. J. Rong, G. Q. Long, G. S. Hu, T. Yan, N. Li, J. M. Jia and A. H. Wang, *Bioorg. Chem.*, 2020, **99**, 103854.

4 L. F. Ding, H. Y. Wang, D. S. Wang, Z. Q. Xie, W. Nie, L. D. Song and X. D. Wu, *Chin. Tradit. Pat. Med.*, 2019, **41**, 840–843.

5 T. Y. Wang, M. Y. Zhao, X. N. Yue, Y. Chen, C. Q. Lu, H. Wang and K. F. Fan, *Chin. J. Exp. Tradit. Med. Formulae*, 2025, **31**, 106–114.

6 F. Wang, X. L. Cheng, Y. J. Li, S. Shi and J. K. Liu, *J. Nat. Prod.*, 2009, **72**, 2005–2008.

7 J. B. Wang, M. H. Wu, C. Gao and H. Z. Fu, *Bioorg. Med. Chem.*, 2019, **27**, 1320–1326.

8 Q. Wu, H. Li, S. Y. Lee, H. J. Lee and J. H. Ryu, *Molecules*, 2015, **20**, 2850–2856.

9 X. D. Wu, L. F. Ding, W. C. Tu, H. Yang, J. Su, L. Y. Peng, Y. Li and Q. S. Zhao, *Phytochemistry*, 2016, **129**, 68–76.

10 J. B. Wang, K. H. Xie, H. Q. Duan, Y. Wang, H. Ma and H. Z. Fu, *Bioorg. Med. Chem. Lett.*, 2017, **27**, 1815–1819.

11 H. Jang, J. W. Lee, J. G. Kim, H. R. Hong, T. P. L. Le, J. T. Hong, Y. Kim, M. K. Lee and B. Y. Hwang, *Bioorg. Chem.*, 2018, **80**, 81–85.

12 S. Schwikkard, A. Alqahtani, W. Knirsch, W. Wetschnig, A. Jaksevicius, E. I. Opara, M. K. Langat, J. L. Andriantiana and D. A. Mulholland, *J. Nat. Prod.*, 2017, **80**, 30–37.

13 Y. Xiang, H. Zhang, C. Q. Fan and J. M. Yue, *J. Nat. Prod.*, 2004, **67**, 1517–1521.

14 R. Wang, W. H. Chen and Y. P. Shi, *J. Nat. Prod.*, 2010, **73**, 17–21.

15 Q. Q. Yuan, W. B. Song, W. Q. Wang, J. J. Wei, J. Li, Y. Liu and L. J. Xuan, *Phytochem. Lett.*, 2017, **21**, 273–277.

16 Z. P. Yu, J. S. Zhang, Q. Q. Zhang, S. J. Yu, Y. Y. Zhang, J. H. Yu and H. Zhang, *Fitoterapia*, 2019, **138**, 104292.

17 X. X. Gao, X. F. Shen, Y. Y. Zheng, L. Y. Yang, X. Y. Zhang, G. S. Hu, J. M. Jia and A. H. Wang, *J. Nat. Prod.*, 2021, **84**, 2808–2821.

18 M. J. Frisch, G. W. Trucks, H. B. Schlegel, G. E. Scuseria, M. A. Robb, J. R. Cheeseman, G. Scalmani, V. Barone, B. Mennucci, G. A. Petersson, H. Nakatsuji, M. Caricato, X. Li, H. P. Hratchian, A. F. Izmaylov, J. Bloino, G. Zheng, J. L. Sonnenberg, M. Hada, M. Ehara, K. Toyota, R. Fukuda, J. Hasegawa, M. Ishida, T. Nakajima, Y. Honda, O. Kitao, H. Nakai, T. Vreven, J. A. Montgomery Jr, J. E. Peralta, F. Ogliaro, M. Bearpark, J. J. Heyd, E. Brothers, K. N. Kudin, V. N. Staroverov, T. Keith, R. Kobayashi, J. Normand, K. Raghavachari, A. Rendell, J. C. Burant, S. S. Iyengar, J. Tomasi, M. Cossi, N. Rega, J. M. Millam, M. Klene, J. E. Knox, J. B. Cross, V. Bakken, C. Adamo, J. Jaramillo, R. Gomperts, R. E. Stratmann, O. Yazyev, A. J. Austin, R. Cammi, C. Pomelli, J. W. Ochterski, R. L. Martin, K. Morokuma, V. G. Zakrzewski, G. A. Voth, P. Salvador, J. J. Dannenberg, S. Dapprich, A. D. Daniels, O. Farkas, J. B. Foresman, J. V. Ortiz, J. Cioslowski and D. J. Fox, *Gaussian 09*, Gaussian, Inc., Wallingford CT, 2013.

19 B. A. Franco, E. R. Luciano, A. M. Sarotti and M. M. Zanardi, *J. Nat. Prod.*, 2023, **86**, 2360–2367.

20 L. Li, H. Z. Qin, S. Lin, H. Zhu and A. D. Wei, *Chin. Tradit. Pat. Med.*, 2023, **45**, 2525–2531.